PUBLICATIONS OF THE ASTRONOMICAL SOCIETY OF THE PACIFIC, **110**:1087–1097, 1998 September

Adaptive Optics Imaging at 1–5 Microns on Large Telescopes: The COMIC Camera for ADONIS

F. LACOMBE AND O. MARCO

Observatoire de Paris, DESPA, F-92195 Meudon, France;
Francois.Lacombe@obspm.fr, Olivier.Marco@obspm.fr

H. GEOFFRAY, J. L. BEUZIT, AND J. L. MONIN

Laboratoire d'Astrophysique, Observatoire de Grenoble, BP 53, F-38041 Grenoble, France;
Jean-Louis.Monin@obs.ujf-grenoble.fr

P. GIGAN AND B. TALUREAU

Observatoire de Paris, DESPA, F-92195 Meudon, France

P. FEAUTRIER AND P. PETMEZAKIS

Laboratoire d'Astrophysique, Observatoire de Grenoble, BP 53, F-38041 Grenoble, France

AND

D. BONACCINI

European Southern Observatory, D-85748 Garching-bei-München, Germany

Received 1998 April 1; accepted 1998 June 17

ABSTRACT. A new 1–5 μm high-resolution camera dedicated to the ESO adaptive optics system ADONIS has been developed as a collaborative project of Observatoire de Paris-Meudon and Observatoire de Grenoble, under ESO contract. Since this camera has been designed to correctly sample the diffraction, two focal plate scales are available: 36 mas pixel^{-1} for the 1–2.5 μm range and 100 mas pixel^{-1} for the 3–5 μm range, yielding fields of view of 4.″5 × 4.″5 and 12.″8 × 12.″8, respectively. Several broadband and narrowband filters are available as well as two circular variable filters, allowing low spectral resolution ($R \sim 60$–120) imagery between 1.2 and 4.8 μm. This camera is equipped with a 128 × 128 HgCdTe/CCD array detector built by the CEA-LETI-LIR (Grenoble, France). Among its main characteristics, this detector offers a remarkably high storage capacity (more than 10^6 electrons) with a total system readout noise of ≈1000 electrons rms, making it particularly well suited for long integration time imagery in the 3–5 μm range of the near-infrared domain. The measured dark current is 2000 electrons s^{-1} pixel^{-1} at the regular operating temperature of 77 K, allowing long exposure times at short wavelengths ($\lambda < 3$ μm), where the performances are readout-noise limited. At longer wavelengths ($\lambda > 3$ μm), the performances are background-noise limited. We have estimated the ADONIS + COMIC imaging performances using a method specially dedicated to high angular resolution cameras.

1. INTRODUCTION

The near-infrared spectral range, from 1 to 5 μm, and more especially from 3 to 5 μm, is the wavelength domain in which thermal emission by warm dust takes place. This wavelength range is therefore a key observational region for addressing numerous astrophysical questions, including the circumstellar environment of young and evolved stars, the dynamics of dust accretion leading to star formation, and the strong emission by active galactic nuclei. But most of these phenomena actually show up at very small angular scale with respect to the resolution that large ground-based telescopes can achieve at infrared wavelengths due to the incoming wave front distortion by the atmospheric turbulence.

To overcome this limitation, adaptive optics (AO) systems have been developed to provide real-time correction of the wave front, hereby restoring the theoretical diffraction-limited resolution of a large ground-based telescope. The first AO system dedicated to astronomy was the COME-ON/COME-ON-PLUS instrument (Rigaut et al. 1991; Rousset et al. 1994). This instrument has recently been upgraded to a new version called ADONIS (Hubin et al. 1993; Beuzit et al. 1994; Beuzit 1994; Demailly et al. 1994; Beuzit, Demailly, & Gendron 1997) and installed on the ESO 3.6 m telescope at La Silla, Chile. Several overviews of astrophysical results have already been published (Léna 1994, 1995; Stecklum 1998).

ADONIS is designed to deliver high angular resolution images in the near-infrared. Diffraction-limited images have al-

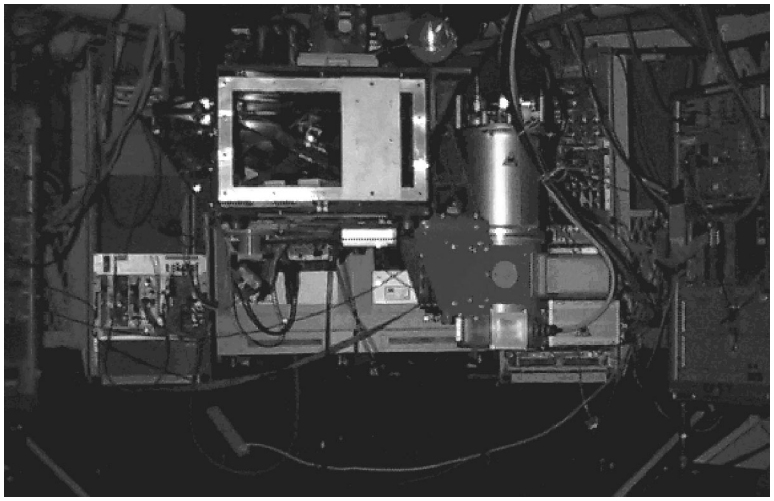

FIG. 1.—Picture of the COMIC camera mounted on the ADONIS optical bench, showing the Dewar, the motors, and the detector electronics

ready been obtained down to 1.7 μm (Rousset et al. 1994) for stars brighter than $m_V = 10$. It is therefore of prime importance to cover the whole near-infrared spectral range with a good imaging system. The 2.5–5 μm domain is of special interest because of its better seeing parameters for the standard atmospheric conditions at La Silla. In order to correctly sample the diffraction-limited images at all wavelengths, the foreseen camera must provide at least 2 pixels in the central Airy disk. The corresponding pixel scale has to be better than 0″.04 in the *J* band, for instance. The camera should also not degrade, by its own optics, the overall image quality. That puts very strong constraints on every individual component. The Dewar itself, as well as the camera mount, should be very stiff and allow typical integration sequences of 1 hr without any detectable displacement of the image on the detector. At worst, in the *J* band, this corresponds to a limit of ~5 mas hr^{-1} for the flexure budget.

In this paper, we present the COMIC infrared camera ded-

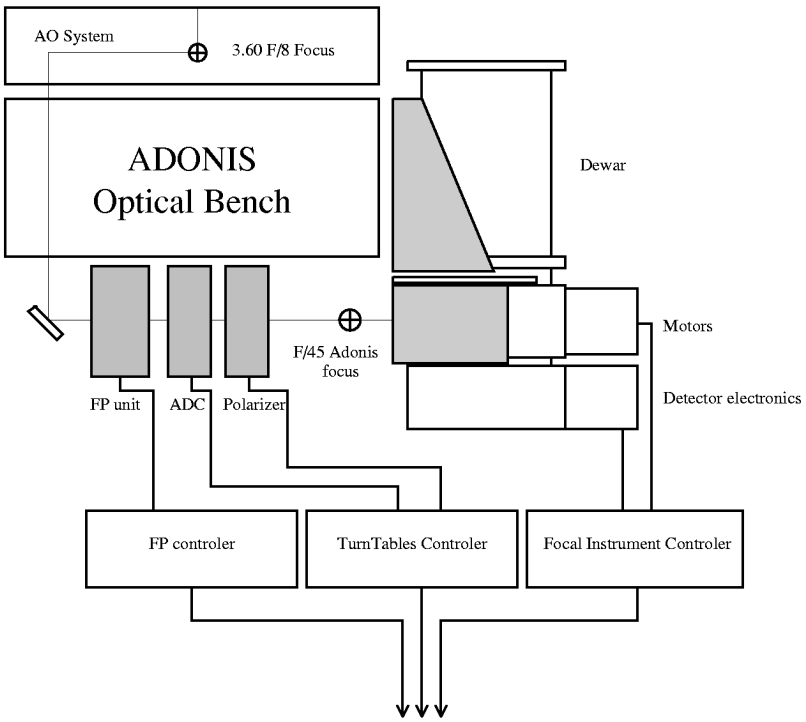

FIG. 2.—Scheme of the COMIC camera, its associated external units, and controllers

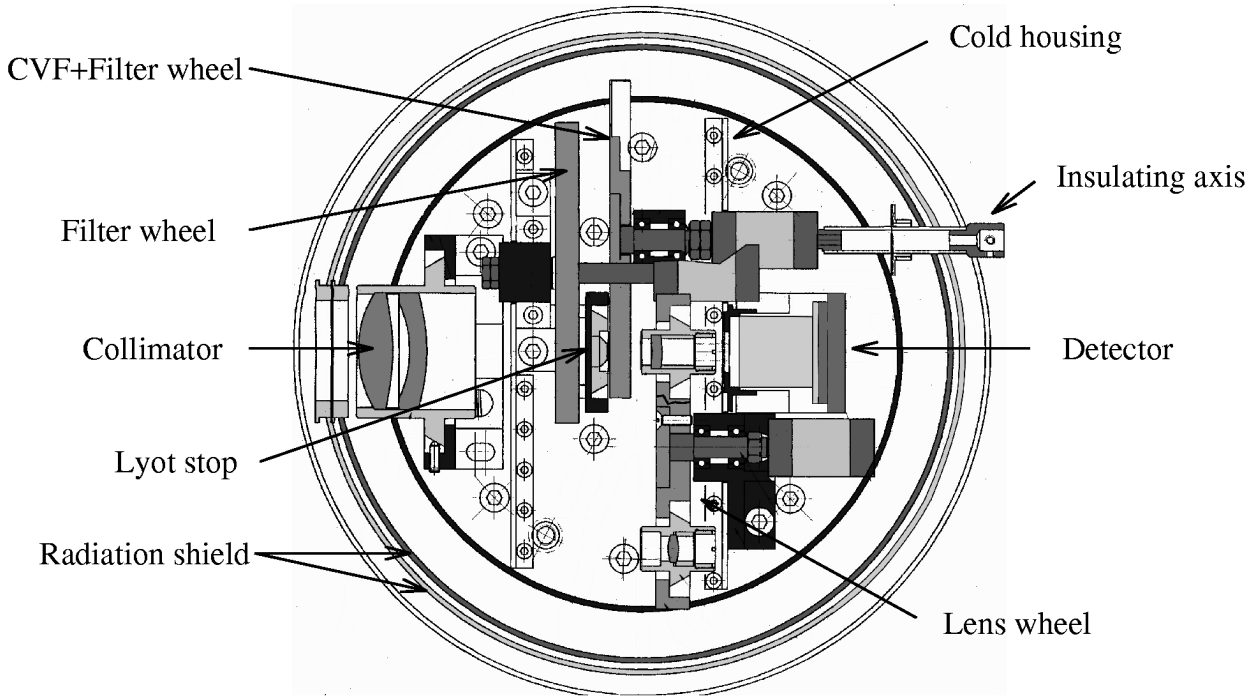

FIG. 3.—COMIC internal optics

icated to the ADONIS system. Section 2 gives a detailed description of the camera subsystems. Section 3 focuses on the detector and its associated electronics, while § 4 presents laboratory calibration results. The COMIC performances are given in § 5, and the first light run is presented in § 6.

2. THE COMIC CAMERA

The COMIC camera (Fig. 1) is mounted at the f/45 output focus of the ADONIS adaptive optics system. It consists of a liquid nitrogen Dewar, which harbors the detector, its relay optics, filters, circular variable filters (CVFs), and several magnification lenses. The detector is sensitive from 1 to 5 μm. Depending on the scientific programs, the camera can be used with two Fabry-Perot units, a polarizer, and an atmospheric dispersion corrector, which are driven by specific controllers located in the telescope Cassegrain cage (Fig. 2).

The global control of the instrument is achieved by a data acquisition system, located in the telescope computer room, which provides the observers with a user interface through which they will configure the camera, control the data acquisition, prepare the real-time processing, or monitor the data storage.

2.1. Optical Design

The internal optics of COMIC consist of two distinct but similar optical trains, respectively optimized for the 1–2.5 and

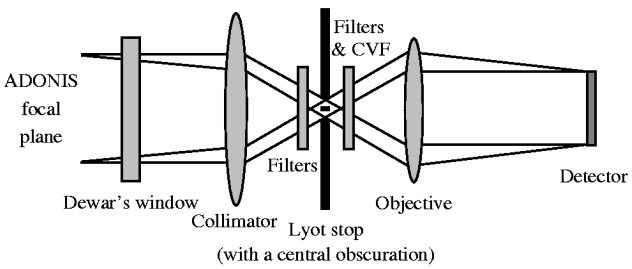

FIG. 4.—COMIC optical design

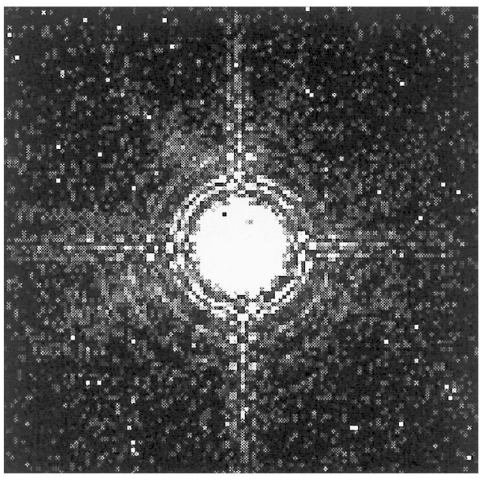

FIG. 5.—Image of a point source at $\lambda = 3.29$ μm (PAH filter) using the long-wavelength objective (field of view: 12″.8 × 12″.8).

3–5 μm spectral ranges (Fig. 3). The optical scheme of COMIC is given in Figure 4. All components, except the cryostat window, are cooled down to 77 K in order to reduce the thermal emission from the optics. A collimator, just behind the Dewar window, images the ADONIS output pupil, located on a chopping mirror, onto a 1.5 mm cold Lyot stop including central obscuration and the spider arms. This small diameter allows low spectral resolution imaging with two circular variable filters ($R \sim 60$ and $R \sim 120$, respectively for the 1.35–2.52 and the 2.50–4.52 μm ranges). Two filter wheels are located close to the pupil image, bearing the two CVFs, seven standard photometric filters, and four narrowband/continuum filter doublets. Then the field is imaged onto the detector, with two possible scales, by means of two objectives, devoted respectively to the 1–2.5 and the 3–5 μm spectral ranges. Both objectives are clamped on a rotating mount that also harbors a pupil imaging lens working at any wavelength. The aim of this lens is to allow a correct alignment of the camera pupil plane with respect to the ADONIS pupil plane. The maximum wave front error is 70 nm rms for the whole optical train.

2.1.1. Lenses

The collimator, a BaF_2/LiF doublet, is achromatic on the whole 1–5 μm range. Due to the low refractive indices of both materials, it has not been antireflection coated at all. The short-wavelength objective (hereafter *J* limit) is made of two BaF_2 lenses, with an antireflective coating on all surfaces and a transmission greater than 98% from 1 to 3 μm. The long-wavelength objective (hereafter *L* limit) is made of one silicon lens, optimized from 3.5 to 5 μm (transmission greater than 98%), with an antireflective coating on both surfaces. At short wavelengths, the 0.″036 pixel^{-1} scale correctly samples a *J* diffraction-limited image, while at longer wavelengths, the 0.″1 pixel^{-1} scale correctly samples an *L* diffraction-limited image (Table 1).

2.1.2. Optical Quality

We present in Figure 5 an image of a point source obtained at $\lambda = 3.29$ μm in the polycyclic aromatic hydrocarbon (PAH) narrowband filter. Because of the high image quality of the camera, numerous diffraction rings (up to 14) can be seen. Note that, due to the central pupil obscuration, successive rings do not have uniformly decreasing luminosity, and only some of them are easily visible (1, 2, 4, 5, 8, 9, etc.).

TABLE 1
CHARACTERISTICS OF BOTH OBJECTIVES

Objective	Plate Scale (arcsec pixel^{-1})	Spectral Range (μm)	Shannon Limit (μm)
J limit	0.036	1.2–3.0	1.2
L limit	0.100	3.0–5.0	3.0

TABLE 2
STREHL MEASUREMENTS OF COMIC ALONE

					CVF		
FILTER	*J* (%)	*H* (%)	*K* (%)	PAH (%)	1.4 μm (%)	1.9 μm (%)	2.4 μm (%)
COMIC Strehl	75	80	89	94	60	64	83

2.1.3. Intrinsic Optical Aberrations

We distinguish between the telescope optical aberrations that are corrected by the AO system and the intrinsic optical aberrations located after the dichroic beam splitter, which separates the visible wavelengths (used for the wave front analysis) from the infrared wavelengths (scientific camera). These static aberrations are due to the ADONIS optical bench optics and the internal COMIC optics. We can measure them using a reference source and thus calibrate the system. Then, applying appropriate offsets to the deformable mirror, we correct for the static aberrations. These static aberrations must be small enough so that there is still room to correct the dynamic aberrations. In other words, the sum of the static and dynamic aberrations must not exceed the capabilities of the deformable mirror. This condition was fulfilled during the technical tests.

We have measured the Strehl ratio for the COMIC camera itself (Table 2) with a white-light monomode fiber source at the Dewar input focal plane. Beyond 4 μm, too much background is present from the fiber holder and Strehl measurement is not precise.

2.1.4. Filters and CVFs

The camera is equipped with standard broadband and narrowband filters as well as two CVFs. Filters and CVFs are mounted on two separate wheels located close to the Lyot stop, in a parallel beam. The characteristics of all filters and CVFs are listed in Tables 3 and 4, respectively.

The filters have been tilted on their supports (~7°) in order to prevent internal reflections that would have led to ghosts. No ghosts are observed with the filters. The CVFs could not be tilted, and we observe a residual image with a flux of about 6% of the real image (Fig. 6).

The wheels of the filters have been deployed so that the thinnest filters (*K*, *L′*, H_2, H_2 continuum, PAH, PAH continuum, H^+_3, H^+_3 continuum, Brα, Brα continuum) are put before the pupil to minimize induced pupil shifts.

2.1.5. Optical Efficiency

The overall efficiency (collimator + objectives + detector) of the COMIC camera at different wavelengths is plotted in Figure 7 for each objective separately. The throughput nonuniformity is due to coatings on the objectives.

TABLE 3
COMIC Broad- and Narrowband Filters

Filter	λ_0 (μm)	$\Delta\lambda$ (μm)	T_{max} (%)
J	1.26	0.23	60
H	1.65	0.33	70
K	2.19	0.41	75
Short *K*	2.16	0.32	75
L	3.48	0.59	80
L′	3.81	0.62	80
M	4.83	0.59	80
H_2 *S*(1)	2.122	0.022	40
H_2 continuum	2.179	0.022	40
PAH	3.290	0.070	50
PAH continuum	3.071	0.240	60
H_3^+	3.534	0.025	40
H_3^+ continuum	3.571	0.025	40
Brα	4.051	0.040	40
Brα continuum	3.775	0.440	60

2.2. Cryostat and Cryomechanisms

Since the COMIC camera is dedicated to high angular resolution astronomy, the cryostat has been designed for both support stability and flexure minimization. To provide a thermal stability all night long at the working temperature of 77 K, the COMIC cryostat has been designed as a two-tank Dewar. Unlike most other liquid cryogen cryostats, in this Dewar, both tanks are directly mounted on the vacuum shell by means of quadripods of glass-reinforced composite, ensuring both a very good stiffness and a sufficient thermal insulation. In addition, the working chamber is located very close to this support (Fig. 8).

As a consequence, the cold optical bench is never misaligned by more than 10 μm, which corresponds to 0.01″ peak-to-peak on the sky, for any orientation of the Dewar. The inner tank holding time is 100 hr for a 2.7 liter liquid nitrogen capacity, and the outer tank hold time is 36 hr for a 4.7 liter liquid nitrogen capacity.

The cryostat is interfaced with the ADONIS bench through a stiff mechanical mount, featuring three translations and two rotations, as required for a correct alignment of the field and the pupil with respect to the AO bench. This mount has proven to keep the cryostat input focus at its theoretical position within a 0.″02 tolerance, while the pupil was not misaligned by more than 5% of its diameter for any position of the telescope.

All cryomechanisms have fine adjustment capabilities in order to align the optics with the required accuracy. The three wheels supporting the filters, CVFs, and objectives are mounted on their supports by means of ball bearings. They are directly driven by external stepper motors (which are fixed on the outer side of the Dewar) in order to limit the internal power dissipation and to simplify the maintenance. A reliable coupling between the motors and the wheels is achieved by vacuum-tight ferrofluidic rotatory feedthroughs and insulating axles. The mechanical resolution is 125 μm for each filter wheel (2000 steps per rotation) and 9.5 μm for the objective wheel (20,000 steps per rotation). All optical elements (except the collimator) as well as the detector itself are enclosed in a light-tight experiment chamber, avoiding light scattering.

TABLE 4
COMIC Circular Variable Filters

CVF	λ_0 (μm)	*R* (%)	T_{mean} (%)
1	1.35–2.52	1.6–1.7	75
2	2.50–4.52	0.8–1.0	65

2.3. Instrument Control

The camera hardware control is achieved by a focal instrument controller, based on a 68,000 VME board. It operates as a slave machine, remotely controlled by the acquisition computer (§ 2.4). In addition to the cryomechanisms hardware control, it also drives the detector readout electronics unit (§ 3) and performs housekeeping tasks such as temperature sensing and bias voltage monitoring.

2.4. Acquisition System: ADOCAM

The COMIC's data acquisition system, ADOCAM, is built around a VME architecture, operating a E7 Eltec's 68040 CPU board under Microware's Os/9 real-time system. Its design and implementation are very similar to the acquisition system of CIRCUS, a speckle infrared camera that the Observatoire de Paris and the Canada-France-Hawaii Telescope have operated routinely at Mauna Kea since 1987 (Lacombe et al. 1989; Gallais 1991). The main feature of the acquisition system is its fully multitasking design that provides modularity and flexibility, allowing any kind of adaptation to a new detector or a new camera. For instance, the SHARP camera (Hofmann et al. 1992) built by the Max-Planck-Institut für Extraterrestrische Physik (Garching, Germany) is driven by ADOCAM as well as by the external units (polarimeter, Fabry-Perot, coronograph, etc.).

Fig. 6.—Image of an extended object with COMIC and a CVF at λ = 3.29 μm (PAH wavelength). The second, fainter, object is a ghost (linear scale).

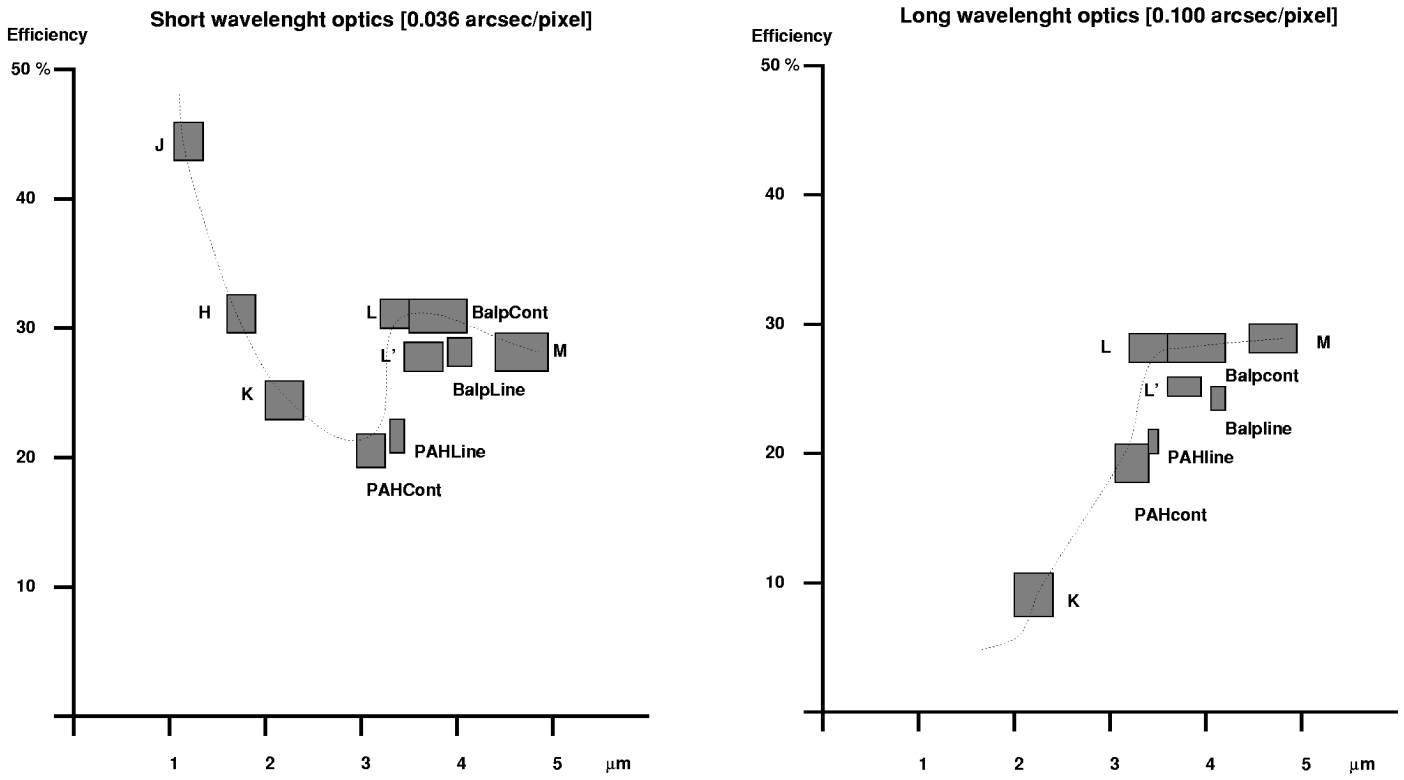

FIG. 7.—Efficiency for all filters with the short-wavelength optics (*left*) and the long-wavelength optics (*right*). The rectangles indicate the bandwidth (horizontally) and the measurement error (vertically).

The acquisition and control computer performs data acquisition, processing, and storage, offers the astronomers a user-friendly X Window interface, and gives a direct control of the cameras (optomechanics and electronics) and the bench (Fabry-Perot, coronograph, Polarizer). This machine is located in the telescope control room together with the ADONIS workstation so that users can get control on the bench and the camera without missing information about the AO system.

The main characteristic of the acquisition system is its ability to organize sequences of observations and not only pure data acquisition. Its connections with the instruments and with the ADONIS workstation make it able to synchronize multiwavelengths observations (filters, CVFs, or Fabry-Perot) with sky emission measurements (chopping) and/or field mosaicking. Once the user has edited these observing sequences, observations are carried out automatically. Saving these configurations allows one to observe several objects or a single object many times in strictly the same way. The relatively low human interaction during automatic observations is somewhat of a guarantee of fewer manipulation errors and higher data quality.

Another important characteristic of the software is its parallelism or multitasking design. Controlling the graphic display while data is being obtained or computing results while raw data are being saved is possible.

2.4.1. Quick-Look Analysis and Display

Once an image is received, real computation starts. This includes sky subtraction, dead pixel processing, flat-fielding, statistics (photometry, signal-to-noise ratio, coherence time, etc.), and shift-and-add, among others. Computation output is then sent to the color display process.

Images are displayed on a private color display (1280 × 1024 pixels) in various ways: color image (zoom available), contour representation (zoom available), isometric three-dimensional representation (zoom available), display of one line and one column as on an oscilloscope, display of one pixel signal versus time. This leads to very high flexibility in the machine/human interaction and to an optimum use of the observing time.

3. THE DETECTOR AND ITS ASSOCIATED ELECTRONICS

3.1. Detector Characteristics

This detector has been extensively described in a previous paper (Feautrier et al. 1994). The COMIC detector is a 128 × 128 HgCdTe photovoltaic focal plane array built by the French manufacturer LETI/LIR in Grenoble. It covers the 1–5 μm spectral range but is more particularly suited for the

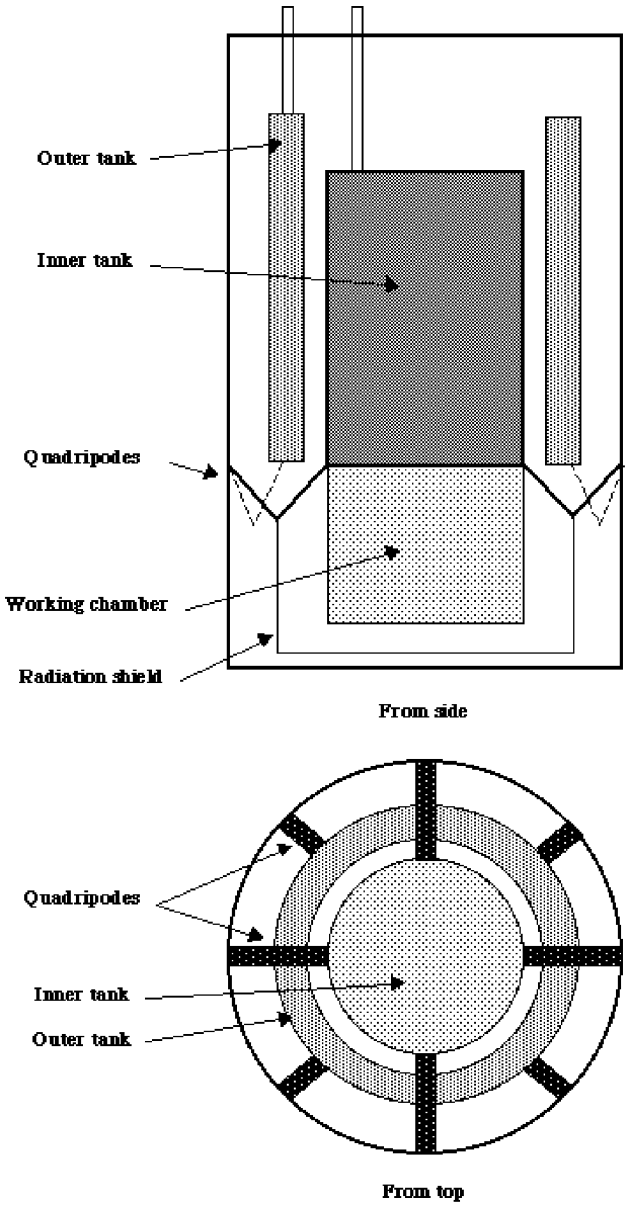

FIG. 8.—COMIC Dewar concept

TABLE 5
MAIN CHARACTERISTICS OF THE COMIC DETECTOR

Characteristic	Description
Manufacturer	LETI/LIR (Grenoble)
Number of pixels	128 × 128
Detection material	HgCdTe
Pixel pitch	50 μm
Filling factor	74%
Cut-off wavelength	5 μm

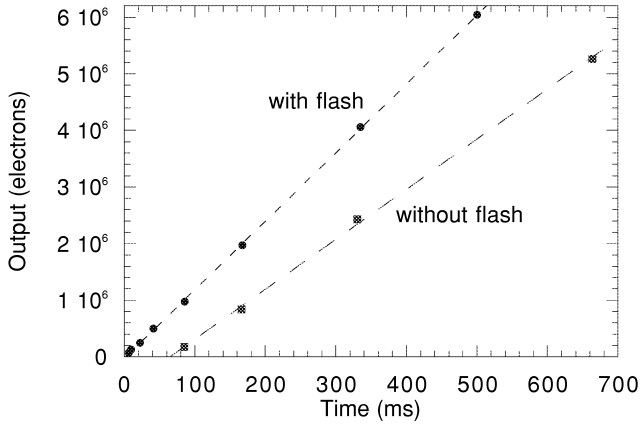

FIG. 9.—Comparison of output with flash and without flash

3–5 μm range. The readout circuitry is a 128 × 128 silicon multiplexer array with one output. The 128 parallel registers are four-phase surface channel CCDs multiplexed by a serial four-phase buried channel CCD. The HgCdTe input diodes are connected to the readout circuit by indium bumps, and the input stages include an antiblooming function. The main characteristics of the COMIC detector are summarized in Table 5.

3.2. Control and Readout Electronics Description

The different functions of these electronics are implemented on six standard "Europe" boards. The boards are integrated in a rack mounted directly onto the Dewar in order to avoid long cables. The detector electronics are designed to provide the following functions:

1. Generation of the detector bias voltages and clocks;
2. Analog-correlated double sampling to filter out the high-

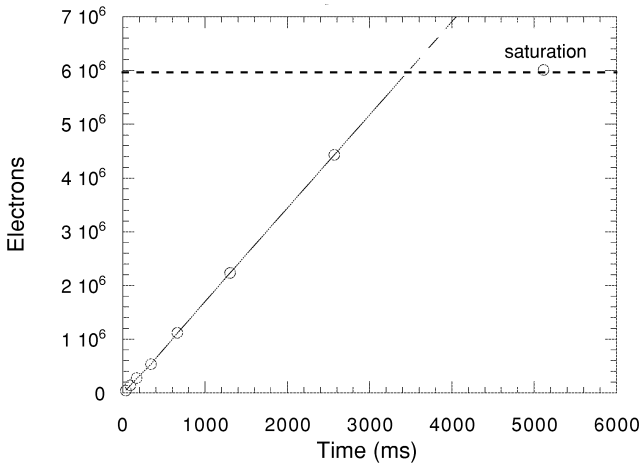

FIG. 10.—Linearity vs. integration time. The saturation level is reached above 6 × 10^6 electrons.

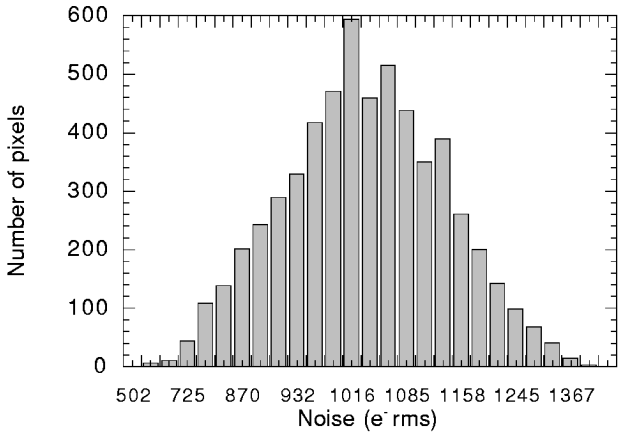

FIG. 11.—Spatial distribution of the global readout noise

frequency noise as well as the low-frequency drift of the CCD output;

3. 16 bit A/D conversion on the same board as the correlated double sampling (the atmospheric dispersion corrector is one of the bottleneck of the readout system, and its maximum pixel rate is of the order of 540,000 samples s^{-1});

4. Serialization and coding of the digitized data to allow transmission through an optical fiber to the data acquisition system located in the telescope control room at a distance of about 40 m;

5. RS232 dialog with the main control system to allow local control and remote commands (integration time setting, voltage bias measurements).

4. CALIBRATION RESULTS

The preliminary performances in terms of readout noise, quantum efficiency, dark current, linearity response, and spatial homogeneity of an engineering model of the LIR detector were measured at Observatoire de Grenoble and at LETI-LIR using a laboratory test bench. All of these results have been reported in a previous paper (Feautrier et al. 1994). Results concerning the science-grade detector, measured in the camera cryostat at Observatoire de Paris, are reported below. The COMIC + ADONIS imaging performance is presented in § 5.

4.1. Dark Current

Adaptive optics cancels the atmospheric phase boiling and allows long integration times. Below 2 μm, due to the reduced thermal emission of the sky and the telescope and due to the spatial dilution of the focal plate scale, the sky background is very low and the dark current becomes one of the main concerns for any detector sensitive in the whole 1–5 μm range. We have measured the detector dark current in the final astronomical Dewar with every potential background source baffled. At 77 K, the average dark current is 2000 electrons s^{-1}. Under low background conditions, the camera is dark-current limited to integration times of about 30 minutes. When used in the 3–5 μm range, the COMIC camera is fully sky-background limited.

4.2. Linearity

We have evidence of a threshold effect at low illumination (Fig. 9). To cancel this effect, we use two diodes to flash the detector during the first 160 μs of the integration time. This flash injects a constant number of charges (800,000), therefore adding about 900 supplementary noise electrons. When used in the 3–5 μm range, this readout noise is negligible compared to the sky background noise.

Then, the overall response curve of the detector versus the integration time is linear (Fig. 10) until a saturation level of about 6×10^6 electrons.

4.3. Readout Noise

After integration in the final astronomical Dewar, preliminary measurements showed a readout noise of 570 electrons rms. When flashing the detector, the global readout noise reaches ~1000 electrons rms (Fig. 11). This readout noise is dominated at long wavelengths ($\lambda > 3$ μm) with broadband filters by the background photon noise (which is greater than 2000 electrons rms).

4.4. Crosstalk

In such a device, the crosstalk between pixels is mainly due to the transfer inefficiency in the serial shift register of the readout CCD. It can be drastically reduced when using appropriate leading and trailing edges for the CCD clocks. After optimization, the averaged serial and parallel crosstalks from one pixel to another have been showed to be less than 1% at 77 K. Therefore, this effect will not degrade significantly the detector performances.

4.5. Quantum Efficiency

The relative detector response has been determined at LETI-LIR. It corresponds to a quantum efficiency of ~60%, roughly constant over the 1–5 μm range.

5. PERFORMANCES OF COMIC

The performance of COMIC is strongly linked to the ADONIS AO system imaging capabilities in the thermal infrared. The AO system was designed to image in the near-infrared, from 1 to 2.5 μm. Subsequently, the COMIC camera was added to extend the AO scientific output (from 3 to 5 μm). But the ADONIS external optics are not cooled, so that there is a thermal background that limits the integration time.

The performance of the COMIC/ADONIS combination should thus be evaluated in terms of both the limiting magnitude and the high angular resolution obtained. In these terms,

this combination produces the best performance for 4 m class telescopes in the 3–5 μm range.

Our method for deriving the imaging performances for a high angular resolution camera separates the various contributions to detectivity loss found in the laboratory and real observing conditions. We chose to estimate the image quality after application of the AO correction by a measure of the Strehl ratio, since this approach can be transferred to any other case, where, for instance, expected seeing values will replace expected Strehl ratios.

5.1. Observations

The first COMIC observing run took place at La Silla observatory in 1995 November. During this technical run, sets of photometrical standard stars were observed in the 1–5 μm spectral range to derive the instrument performances.

Considering the detector characteristics, we adjusted the integration time per frame so that observations could be background-noise limited (BLIP conditions) whenever possible, i.e., at long wavelengths. Knowing that at short wavelengths the detector readout noise would be the limiting noise source, we increased the integration time to 30 s. Since we are limited by readout noise, we had to increase the exposure time, rather than averaging images, in order to increase the signal-to-noise ratio (S/N). In order, however, to detect any possible fluctuations in the AO correction, we could not use too long of an exposure time. The choice of exposure time was thus a compromise between these two constraints.

To accurately trace background fluctuations at all wavelengths, we used a chopping method of observations. This method alternates between observations of the object and observations of the background. In order to accomplish this, we use a so-called ONOFF mirror located on the ADONIS imaging channel. This mirror selects a field of view of 12″.8 × 12″.8 (with the high wavelength objective) from within a total field of 30″ × 30″.

During our study, we chose a three-positions chopping pattern, consisting in one on-the-object position flanked by two symmetrical off-the-object positions. This three-positions chopping technique is known to be, in infrared photometry, one of the most efficient to derive a correct estimate of the instrument or sky background whenever no guarantee can be made to ensure a total background homogeneity, as was the case for this first observing run with ADONIS in the thermal domain.

From the analysis of these data we can then derive instrument metrics, such as Strehl ratio, FWHM, conversion factor (zero point), or limiting magnitude, without making any assumption about the type of limiting residual noise, be it readout noise, background photon noise, or background macroscopic but spatially uncorrelated noise.

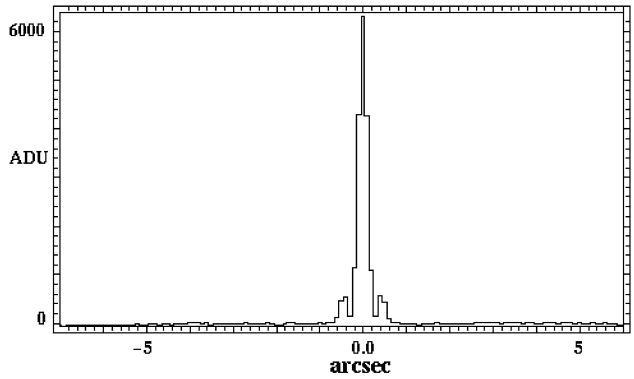

FIG. 12.—Cut of the bright star HR 8720 in the *M* band with ADONIS and COMIC. The Strehl ratio is 61% for an integration time of 0.5 s.

5.2. Deriving the Performance

At short wavelengths, the readout noise dominates the background noise. In that case, we increase the detector integration time as much as possible before adding pictures. At long wavelengths, we observe under background-limited performances (BLIP), and the S/N increases as $n^{1/2}$, where n is the total number of observed frames. A detailed calculation has been presented in Marco, Lacombe, & Bonaccini (1996) and can be found also in Marco (1997).

We present in Table 6 the observed limiting magnitude for two kinds of sources, unresolved and extended, under realistic observing conditions for an equivalent integration time of 900 s and an S/N equal to 5.

6. PRELIMINARY RESULTS

6.1. First Light on COMIC

Figure 12 clearly demonstrates the excellent imaging quality of ADONIS with the COMIC camera on the star HR 8720: the value of the Strehl ratio is up to 60% and the diffraction

TABLE 6
LIMITING MAGNITUDES

Band	*J*	*H*	*K*	*L*	*L′*	*M*
Angular resolution (arcsec)	0.09	0.12	0.15	0.24	0.27	0.34
Extended object (mag arcsec^{-2})	9.3	9.4	9.0	8.6	8.2	6.3
Unresolved object (mag)	13.0	12.5	11.8	10.7	10.1	7.7

NOTE.—Calculated for S/N = 5, T_{eq} = 900 s.

TABLE 7
SUMMARY OF COMIC CALIBRATION MEASUREMENTS

Characteristic	Value
Number of pixels	128 × 128
Detection material	HgCdTe
Pixel pitch	50 μm
Filling factor	74%
Cutoff wavelength	5 μm
Frame readout time	40 ms
Storage capacity	6×10^6 electrons
Total readout noise at 410 kHz	1000 electrons rms
Quantum efficiency (1–5 μm)	60%
Dark current at 77 K	2000 electrons s^{-1}
Crosstalk pixel/pixel	1%

limit is achieved, in the *M* band, under average seeing conditions (not better than 1.″5).

6.2. Pre–Main-Sequence Binary Stars

Figure 13 shows the *L* band image of a pre–main-sequence (PMS) binary, together with the reference point-spread function (PSF) star, obtained with COMIC in 1996 May (Monin, Geoffray, & Ménard 1997). The images have been flat-fielded and corrected for bad pixels, but no deconvolution has been applied. Although the image correction is not complete, two diffraction rings are clearly visible on the image and on the PSF reference star. The *L* magnitudes of the binary components are 7.1 and 8.2, respectively, and the separation is 0.″5. The observations have been obtained with an individual frame integration time of 1 s.

We have compared the noise on the background of the images with the amplitude of the signal on the star, and from these first observations, we can conservatively conclude that COMIC can detect an $L = 11$ star in 1 s with an S/N of 1. If we scale the results of table to 1 s/1 σ, the limiting *L*-band magnitude should be $L = 11.9$. Those two estimations are thus very consistent.

7. CONCLUSIONS

We have developed an infrared high angular resolution camera to be used on the ADONIS adaptive optics system. The preliminary laboratory results, summarized in Table 7, demonstrate that this camera is well suited for imaging with adaptive optics in the 3–5 μm spectral range, where its performance is sky-background limited. New software, including real-time facilities such as shift-and-add, dead pixel removal, sky subtraction and flat fielding, statistics (S/N, histogram, diaphragm photometry), three-dimensional view, zoom, one pixel versus time, batch sequences, and automatic logbook, allows evaluation and improvements in real time of the scientific output of observations.

The performance of the COMIC camera, as measured during the qualification tests in Grenoble and Meudon, then during the technical run in 1995 November, shows that this camera, in conjunction with the AO system ADONIS, is fully adapted to imaging operation in the 3–5 μm spectral band. The large dynamic range of the detector (with a low dark current) allows long exposure time imaging at all wavelengths, which is made possible by the improvements in image quality provided by the AO system. We achieved diffraction-limited performances on a 3.6 m telescope in the 1–5 μm observation band, thus giving an angular resolution ranging from 0.09″ (*J* band) to 0.34″ (*M* band). The COMIC camera has been fully operational on ADONIS since 1996 March.

We thank Pierre Léna, who initiated this project, and Daniel Amingual and the LETI-LIR staff for their constant support. This project was carried out under ESO contract 38082/ESO/TEL/92/7040/GWI. It also received financial support from the Ministère de la Recherche et de l'Enseignement Supérieur, from the Centre National de la Recherche Scientifique (URA 264 and UMR 5571), and from the Direction des Recherches, Etudes et Techniques (contract 94-1056/A000/DRET/DS/SR). H. G. acknowledges partial financial support from SOFRADIR. We also thank Antony Seward for his fruitful comments on this paper and David Le Mignant and Franck Marchis for operating COMIC.

FIG. 13.—First COMIC *L*-band (3.5 μm) image of a PMS binary (*left*) together with its associated PSF reference star (*right*). The binary separation is 0.″5, and the FWHM is 0.″24 (diffraction limit).

REFERENCES

Beuzit J. L. 1994, Ph.D. thesis, Univ. Paris 6
Beuzit, J. L., et al. 1997, Exp. Astron., 7, 285
Beuzit J. L., et al. 1994, Proc. SPIE, 2201, 955
Demailly, L., Gendron, E., Beuzit, J. L., Lacombe, F., & Hubin, N. 1994, Proc. SPIE, 2201, 867
Feautrier, P., Geoffray, H., Petmezakis, P., Monin, J. L., Le Coarer, E., & Audaire, L. 1994, Proc. SPIE, 2268, 386
Gallais, P. 1991, Ph.D. thesis, Univ. Paris 7
Hubin, N., Rousset, G., Beuzit, J. L., Boyer, C., & Richar, J. C. 1993, Messenger, 71, 50
Hofmann, R., et al. 1992, in Progress in Telescope and Instrumentation Technologies, ed. M.-H. Ulrich (Garching: ESO), 687
Lacombe, F., Tiphène, D., Rouan, D., Léna, P., & Combes, M. 1989, A&A, 215, 211
Léna, P. 1994, Proc. SPIE, 2201, 1099
———. 1995, in Science with the VLT, ed. J. R. Walsh & J. Danziger (Berlin: Springer)
Marco, O. 1997, Ph.D. thesis, Univ. Paris 6
Marco, O., Lacombe, F., & Bonaccini, D. 1996, Messenger, 85, 39
Monin, J. L., Geoffray, H., & Ménard F. 1997, in IAU Symp. 182, Herbig-Haro Flows and the Birth of Low-Mass Stars, ed. J. Provost & F.-X. Schmieder (Dordrecht: Kluwer), 230
Rigaut, F., et al. 1991, A&A, 250, 280
Rousset, G., et al. 1994, Proc. SPIE, 2201, 1088
Stecklum, B. 1998, Proc. SPIE, in press